Fate of Organic Matter over Geologic Time

Reading list

Any general petroleum geochemistry text book

Killops S.D. and Killops V.J. (1993) *An introduction to Organic Geochemistry*. 265 pp. Longman

Hunt J.M. (1996) *Petroleum Geochemistry and Geology*, 2nd Edition. Freeman and Co. San Francisco.

Tissot and Welte (1984) *Petroleum formation and occurrence*. Springer-Verlag, New York, 699 pp.

Engel M.H. and Macko S.A. (1993) *Organic Geochemistry: Principles and Applications*. Plenum Press, NY

Peters K.E. and Moldowan J.M (1993) *The Biomarker Guide*. Prentice Hall.

Organic sulfur geochemistry

Francois R. (1987) A study of sulfur enrichment in the humic fraction of marine sediments during early diagenesis. *Geochim. Cosmochim. Acta* **51**, 17-27.

Sinninghe Damste J.S., Rijpstra W.I.C., Kock-van Dalen A.C., de Leeuw J.W. and Schenck P.A. (1989) Quenching of labile functinalized lipids by inorganic sulfur species: Evidence for the formation of sedimentary organic sulfur compounds at an early stage of diagenesis. *Geochim. Cosmochim. Acta* **53**, 1433-1455.

Sinninghe Damste J.S., Kok M.D., Koster J., and Schouten S. (1998) Sulfurized carbohydrates: an important sedimentary sink for organic carbon? *Earth Planet. Sci. Lett.*, **164**, 7-13.

Werne J.P., Hollander D.J., Behrens A., Schaeffer P., Albrecht P. and Sinninghe Damste J.S. (2000) Timing of early diagenetic sulfurization of organic matter: A precursor-product relationship in Holocene sediments of the Cariaco Basin, Venezuela. *Geochim. Cosmochim. Acta* **64**, 1741-1751.

The Global Organic Carbon Cycle (ca. 1950)

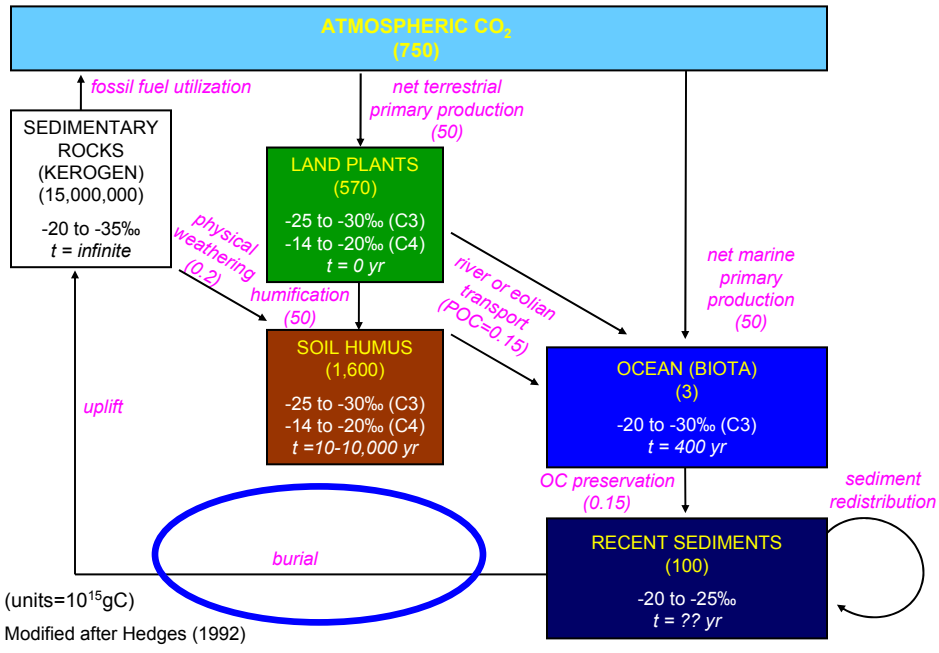

Biogeochemical Sedimentary Sulfur Cycle

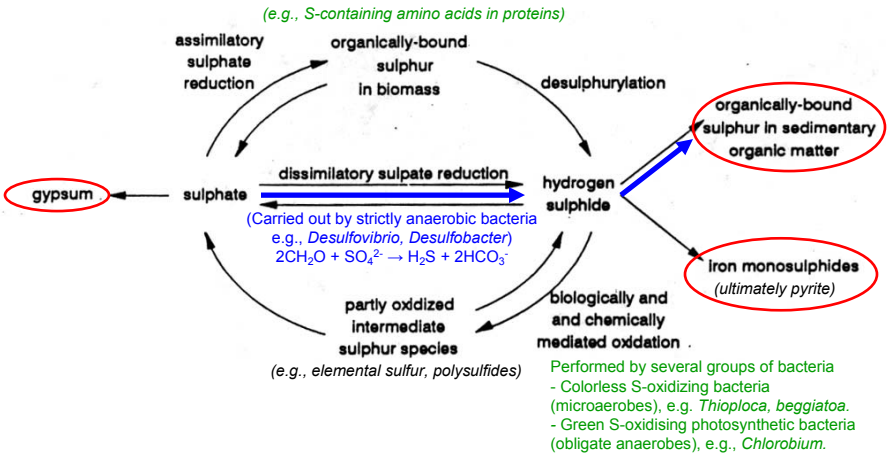

= sinks

- Precipitation of gypsum ($Ca_2SO_4.2H_2O$)
- Reaction of hydrogen sulfide with reactive iron minerals to form monosulfides (FeS) and pyrite (FeS_2)
- *Reaction of reduced sulfur species (e.g. H_2S) with organic matter leading to formation of organically-bound sulfur in sediments.*

Early diagenetic incorporation of sulfur into organic matter

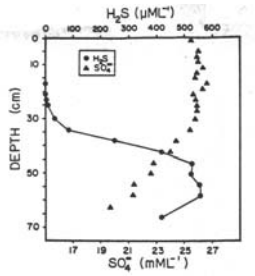

Fig. 5. Pore waters sulphide and sulphate concentrations (data from Core A).

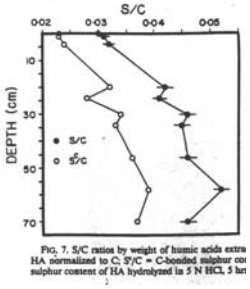

Fig. 7. S/C ratios by weight of humic acids extra HA normalized to C. S/C = C-bonded sulphur co sulphur content of HA hydrolyzed in 5 N HCl, 5 hr

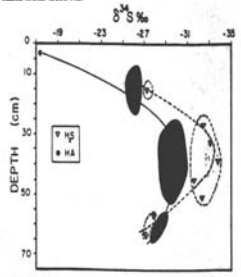

Fig. 8. Isotope composition of free sulphides (H_2S) and hydrolyzed humic acids (HA) (data from Core B).

Francois, 1987

Peru "kerogens"

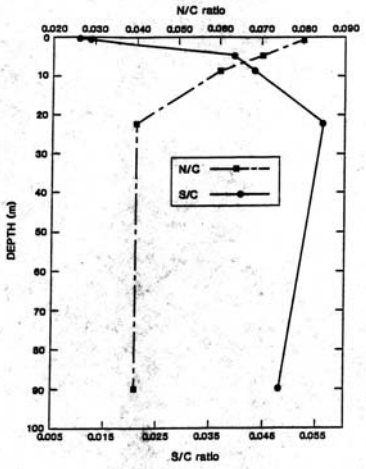

Patience et al., 1990

Formation of organically-bound sulfur in sediments

- Studies of gross elemental composition of organic matter provide strong evidence that the majority of organically-bound sulfur in sediments is the result of an abiogenic reaction of reduced sulfur species with organic matter during the early stages of diagenesis.
- Mass balance calculations and sulfur isotopic analysis indicates that biogenic sulfur (e.g. proteins such as cysteine, methionine) is a negligible component of organically-bound sulfur in sediments.
- It is generally considered that reactive iron species (e.g. ferrihydrite, haematite) out-compete organic matter for reduced sulfur species because OM reacts more slowly than do detrital Fe minerals.
- The onset of "sulfurization" of organic matter therefore controlled by reactive Fe content. Commences after conversion of reactive iron oxides to iron sulfides.

Mechanism for formation of OSC

- Lipids and carbohydrates appear to be major targets for sulfur attack
- The position of sulfur linkages is related to the positions of former functional groups (e.g. double bonds) in precursor compounds

Sulfur species reacting with OM

- Three major sulfur species believed to be possible reactants with OM:
  - H_2S (Nissenbaum and Kaplan, 1972)
  - Polysulfides (Aizenshtat et al., 1983; Lalonde et al., 1987)
  - Elemental sulfur
- The majority of compounds identified are consistent with H_2S as major reactant
- Kohnen et al. (1989) identified C_{20} isoprenoid compounds with heterocycles containing two or three sulfur atoms. Implies incorporation of inorganic polysulfides

Proposed mechanism of OSC formation

- Addition of H_2S (or other reduced sulfur species) to double bonds or other functionalities.
- Vairavamurthy and Mopper (1987) provided evidence for formation of 3-mercaptopropionic acid (virtually ubiquitous in coastal marine sediments) from abiotic reaction between hydrogen sulfide and acrylic acid (a cleavage product of the common algal osmolyte, β-dimethyldisulphoproprionate).
- Fukushima et al. (1991) performed simulation experiments using phytol and hydrogen sulfide in aqueous solution at close to ambient temperatures and produced C_{20} alkylthiophenes.

Early diagenetic formation of thiols in sediment pore-waters

Biscayne Bay, Florida

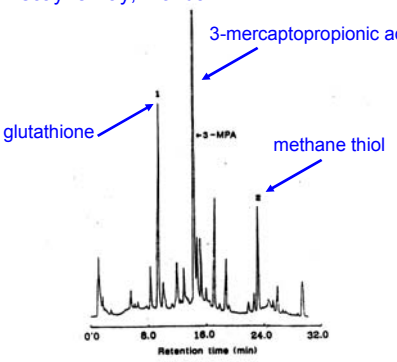

Fig. 1 A typical chromatogram of thiols in a sediment pore-water sample (Biscayne Bay, Florida) using high-performance liquid chromatography pre-column *o*-phthalaldehyde derivatization and fluorescence detection. Peaks numbered 1 and 2 correspond to glutathione and methane thiol respectively.

CH_2=CHCOOH + HS^- → $HSCH_2CH_2COOH$

acrylic acid — 3-mercaptopropionic acid

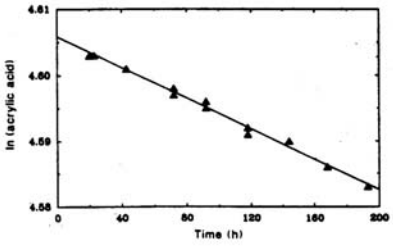

Fig. 2 Pseudo first-order reaction kinetics for the formation of 3-MPA with excess bisulphide (5 mM) and limiting acrylic-acid concentrations. The reaction was carried out in de-aerated, filter-sterilized sea water (salinity 35 and *p*H 8.4) at 23 °C. Acrylic acid concentrations were calculated by subtracting the amount reacted to form 3-MPA from the starting concentration. The straight line had an equation; $y = -0.00011$; x, $+4.6058$ and $r^2 = 0.993$ (r^2 is the coefficient of determination).

Vairavamurthy & Mopper, 1987

Depositional settings favoring the formation of sulfur-rich sedimentary OM

Depositional env.	**Contemporary**	**Ancient**
Carbonate platforms	Blake Bahama Plt.	Brown Limestone Fm.
Evaporites	Abu Dhabi	Mediterranean
Upwelling systems	Peru Margin	Monterey Fm.
Restricted marine basins	Black Sea	Kimmeridge Fm.

Modes of formation of OSC

Two possible modes of OSC formation: *Intra*- and *Inter*-molecular addition:

Intramolecular sulfur incorporation/addition

- Reaction of sulfur within a single molecule to form acyclic or cyclic sulfur compounds

Intermolecular sulfur incorporation

- Reaction of sulfur between molecules giving rise to sulfur linkages or bridges.
- These reactions provide a pathway for the formation of large macromolecules through sulfur bridges (cross-linking).
- This has been proposed as a mechanism for kerogen formation in sediments (Sinninghe Damste et al. 1989; Kohnen et al. 1991).

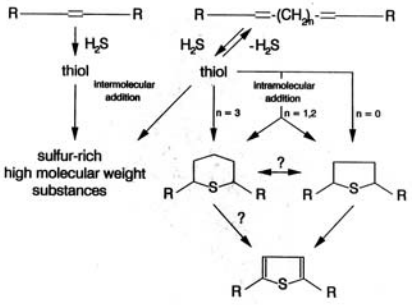

Molecular-level evidence for abiotic formation of Organic Sulfur Compounds (OSC) in sediments

- Identification of a C_{35} hopanoid thiophene in immature Cretaceous black shales (Valisolalao et al. 1984)
- Inferred origin: reaction of sulfur with bacteriohopane tetrol.
- Identification of C_{20} isoprenoid alkylthiophenes in immature sediments and crude oils (Brassell et al., 1986; Sinninghe Damste et al., 1986; Rullkotter et al., 1988)
- Inferred origin: reaction of sulfur with chlorophyll derived phytol.
- Now many hundreds of OSC have been identified with very strong product-precursor relationships.

Bacteriohopane tetrol

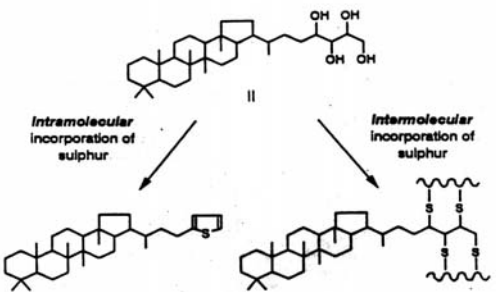

Formation of organic sulfur compounds

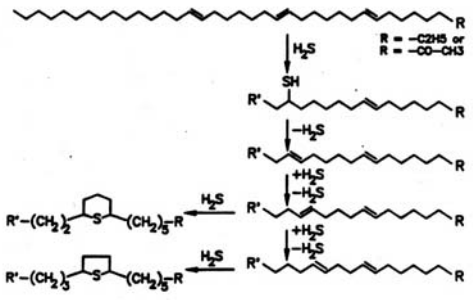

Reaction with $C_{37:3}$ ketone

Reaction with C_{25} HBI alkene

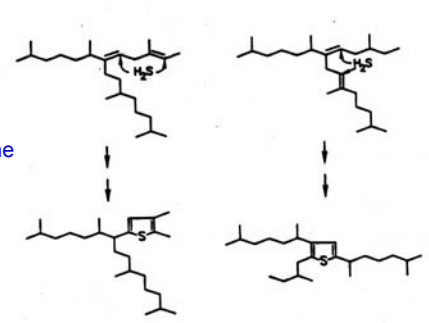

Evidence for reaction of polysulfides with OM

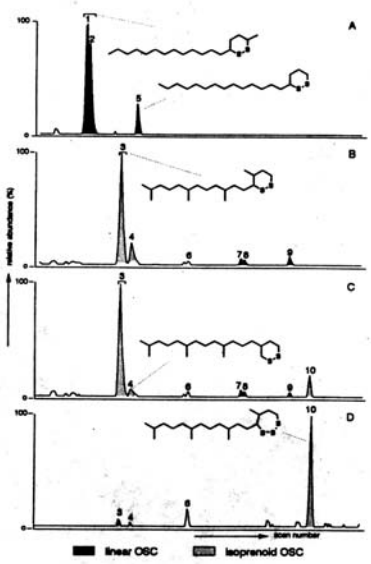

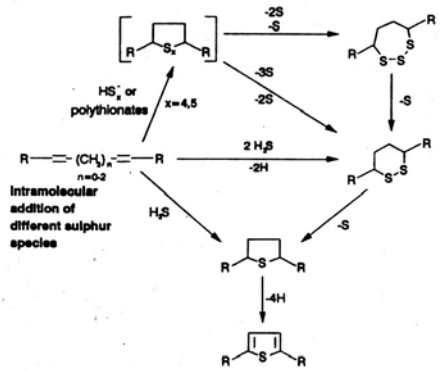

Kohnen et al.

Organic sulfur formation in Cariaco Basin sediments

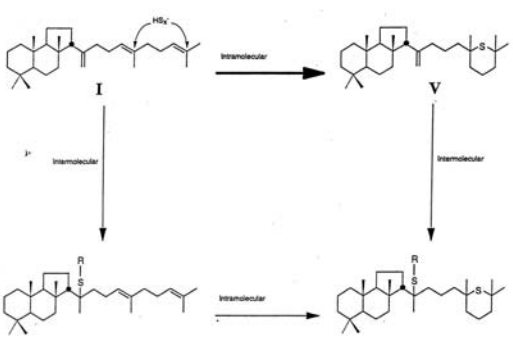

Fig. 4. Reaction scheme for incorporation of inorganic sulfur species into (17*E*)-13*β*(*H*)-malabarica-14(27),17,21-triene (I). The most likely pathway is intramolecular sulfurization at the Δ^{17} and Δ^{21} double bonds, followed by intermolecular sulfurization at the 14(27) double bond.

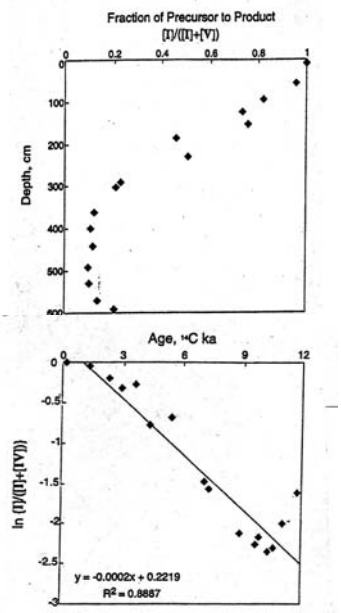

Werne et al. 2000 GCA 64, 1741-1751

Possible relationship between sulfur cross-linking and molecular size of organic matter

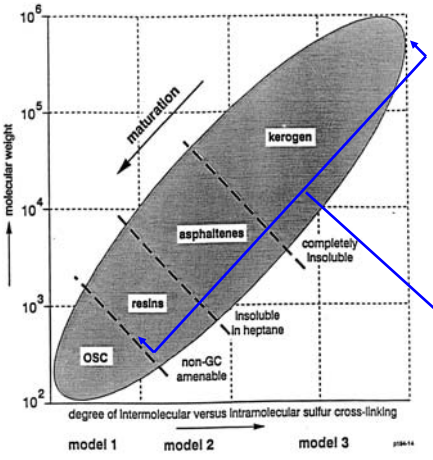

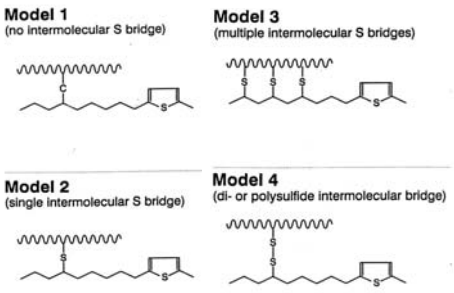

Analysis of macromolecularly bound S in sediments
- Analytical pyrolysis
- Selective chemical degradation methods
- X-Ray spectroscopy
- Sulfur Isotopic Analyses

Pyrolysis-GC of Peru kerogens

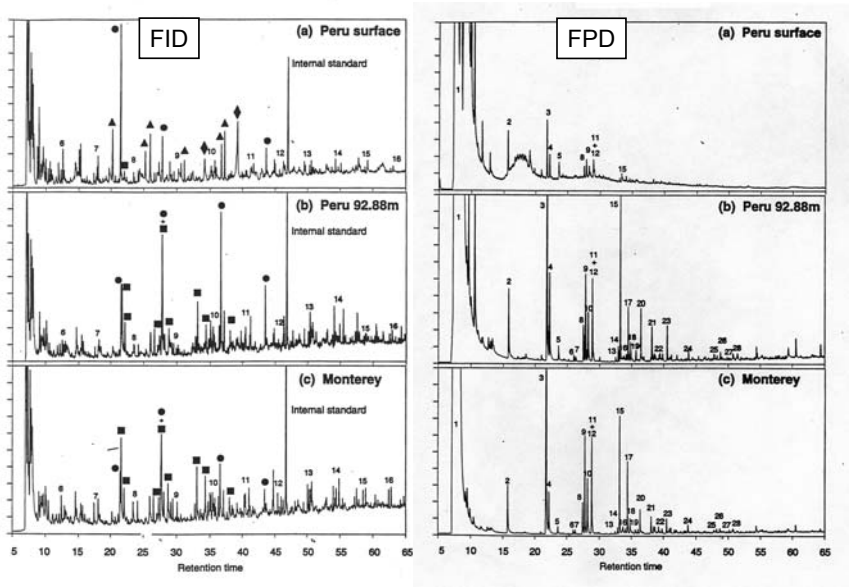

Sulfurization of polysaccharides

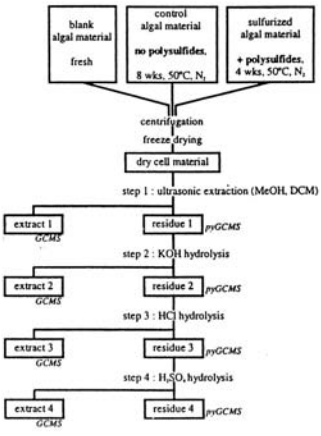

Fig. 1. Analytical scheme.

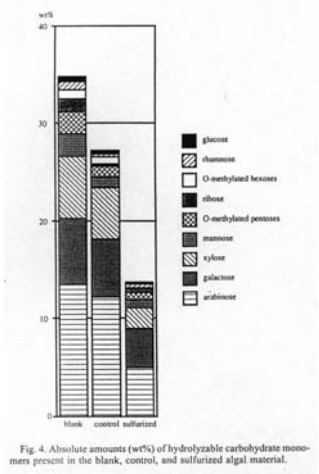

Fig. 4. Absolute amounts (wt%) of hydrolyzable carbohydrate monomers present in the blank, control, and sulfurized algal material.

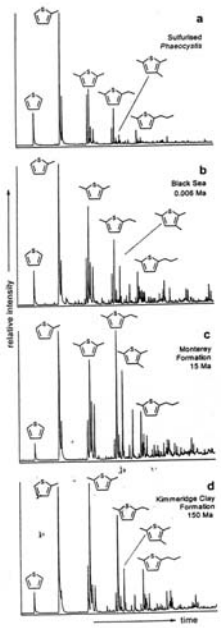

Sinninghe Damste et al. 1998 EPSL 164 7-13

Importance of organically-bound sulfur

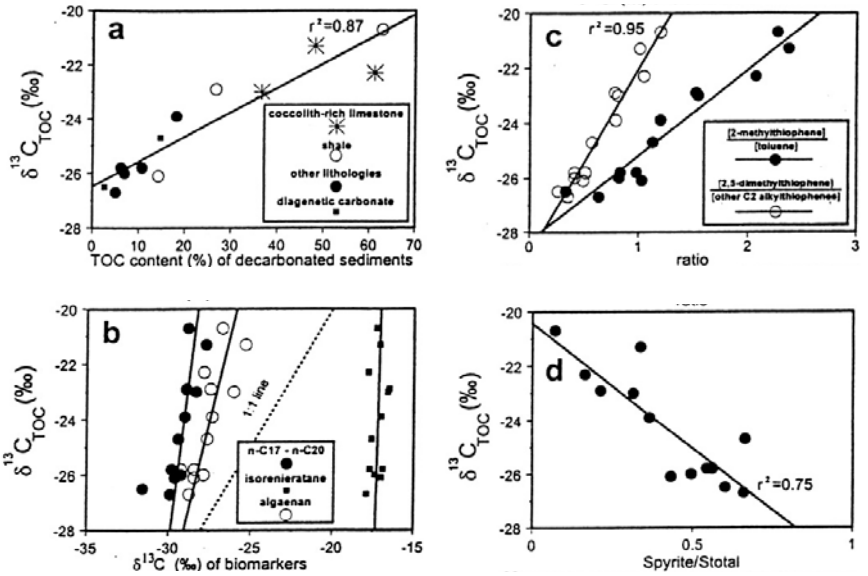

Sinninghe Damste et al. 1998 EPSL 164 7-13

Sulfur-selective chemical degradation methods

	Raney Ni/H_2	MeLi/MeI
Principle		
R_1-S-R_2	R_1-H + R_2-H	No Products
R_1-S-S_n-S-R_2 ($n \geq 0$)	R_1-H + R_2-H	R_1-S-CH_3 + R_2-S-CH_3
R-SH	R-H	R-S-CH_3
Examples		
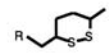	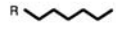	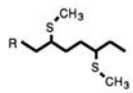
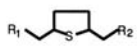		No Products
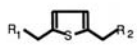		No Products

Modes of occurrence of phytane carbon skeleton

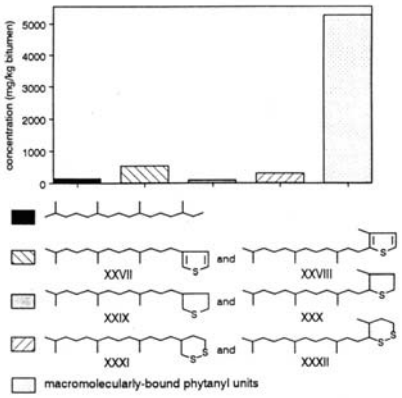

Figure 7.8. The distribution of the phytane carbon skeleton over the different modes of occurrence in the Vena del Gesso Marl-7A3. It is evident that the major portion of the amount of phytane carbon skeletons is present as macromolecularly sulphur-bound moieties. Di- or polysulphide bound phytanyl moieties with the sulphur-linkages at C-1, C-2, C-3, C-4 and C-17 comprise *ca. 40* wt.% of all macromolecularly sulphur-bound phytanyl moieties and the the ones with the sulphur-linkage located at C-3 are by far dominant (*ca.* 80 wt. %). The particular compounds were analysed quantitatively by GC using internal standards as described previously (Kohnen et al., 1990c).

Sequestration of organic compounds via reaction with sulfur

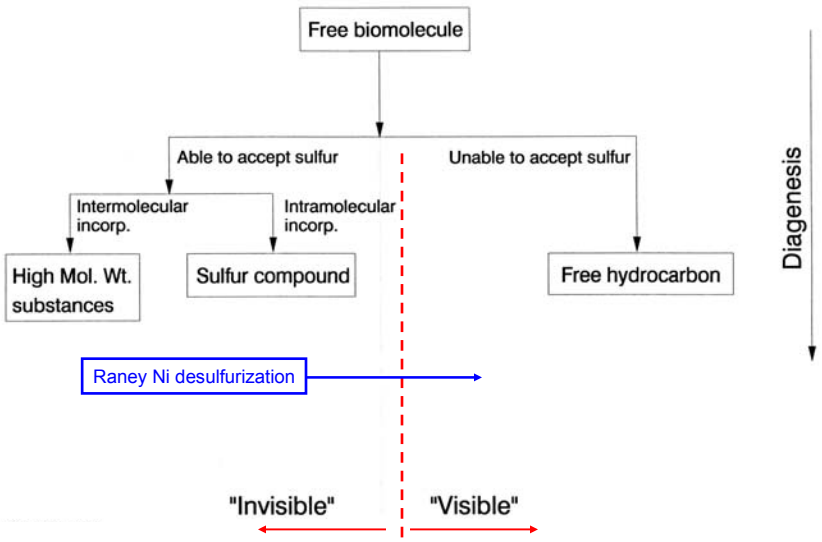

Biases in biomarker records due to formation of organically-bound sulfur

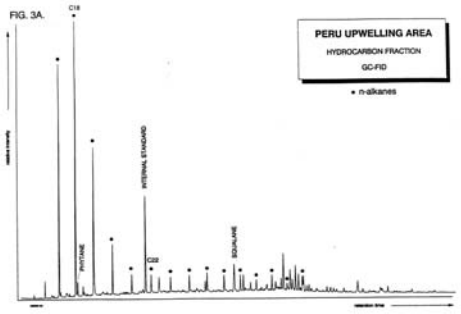

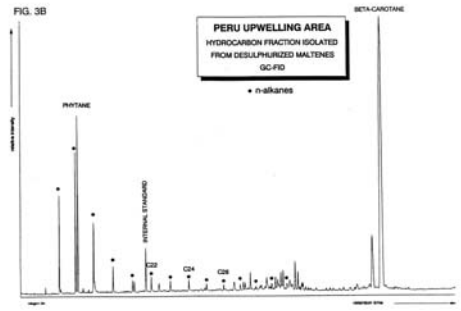

Sulfur X-Ray absorption spectroscopy

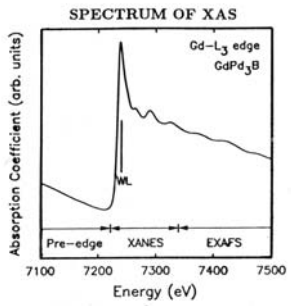

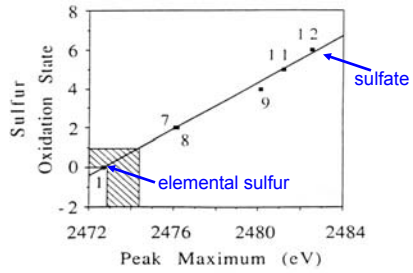

Absorption	Transition
K	$1s \longrightarrow np$
L_1	$2s \longrightarrow np$
L_2	$2p_{1/2} \longrightarrow nd_{3/2}, nd_{5/2}$
L_3	$2p_{3/2} \longrightarrow nd_{5/2}$

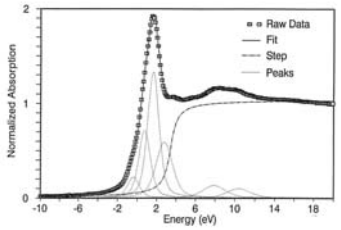

Sulfur speciation in Peru margin sediments

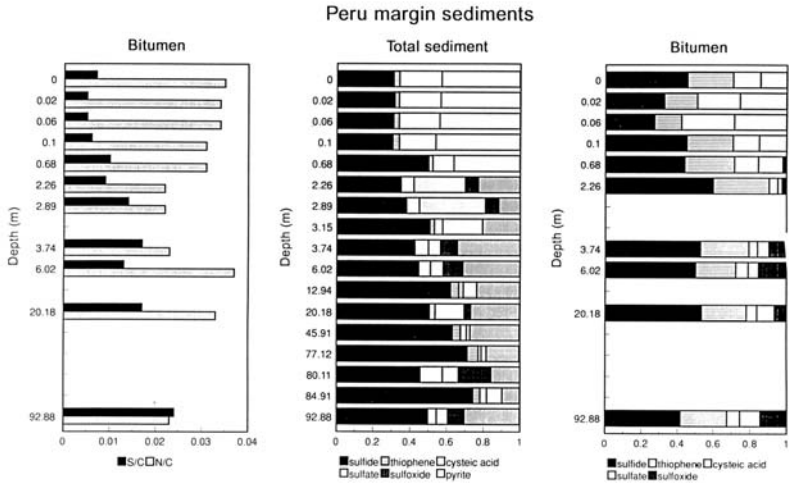

Figure 1. Bulk geochemical analyses of Peru margin sediments: Atomic S/C and N/C ratios determined for total solvent extracts (left); sulfur speciation determined by XANES for total sediment (center) and solvent extracts (right). Speciation is defined according to best-fit calculations with respect to standard compounds (dibenzylsulfide, dibenzothiophene, cysteic acid, benzyl sulfoxide, sodium sulfate and pyrite).

Geochemical Implications of Organically-bound Sulfur

- Role of anoxia in organic carbon preservation.
- Importance as a sink for sulfur (may have been more significant in geologic past).
- Potential biases in interpretation of lipid biomarker distributions as a result of natural sulfurization.
- Influence on the timing of petroleum generation
- Influence on petroleum composition

O_2-depleted environments associated with deposition of OC-rich sediments

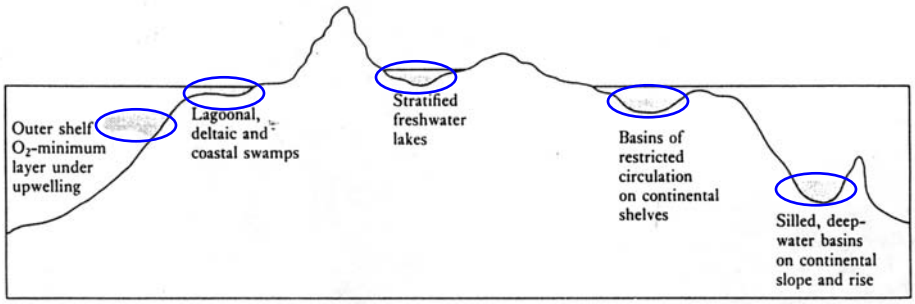

Marine and lacustrine benthic environments

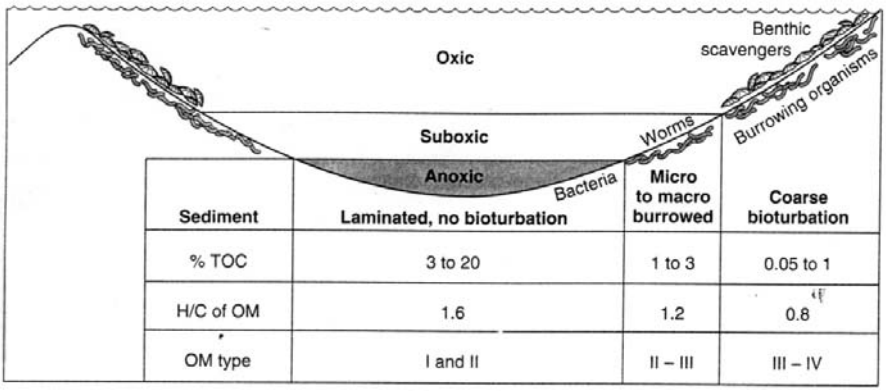

Sediment	Laminated, no bioturbation	Micro to macro burrowed	Coarse bioturbation
% TOC	3 to 20	1 to 3	0.05 to 1
H/C of OM	1.6	1.2	0.8
OM type	I and II	II – III	III – IV

Figure 5-1

Marine and lacustrine benthic environments. Oxygen contents in ml/l H_2O are oxic greater than 1, suboxic 1 to 0.1, and anoxic less than 0.1 OM. Types I to IV are defined in Chapter 6.

Fossil fuel reserves and source rock age

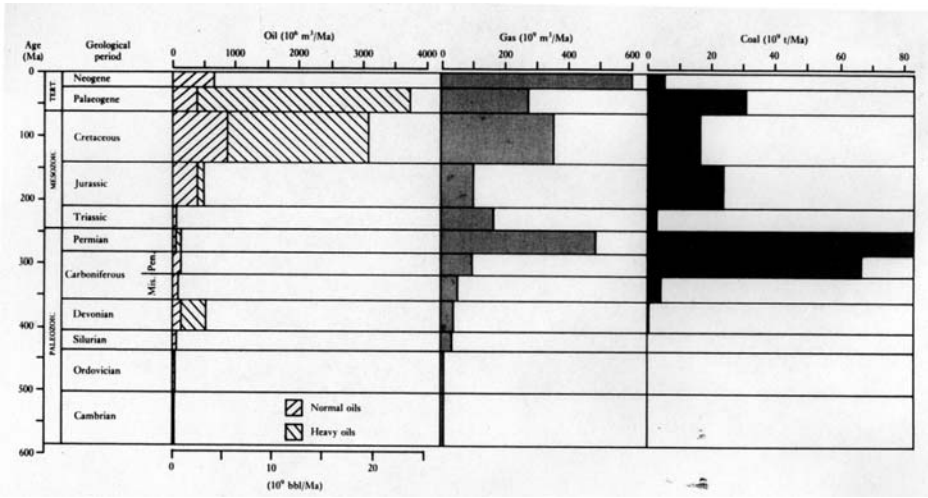

Evolution of important sedimentary organic matter precursors

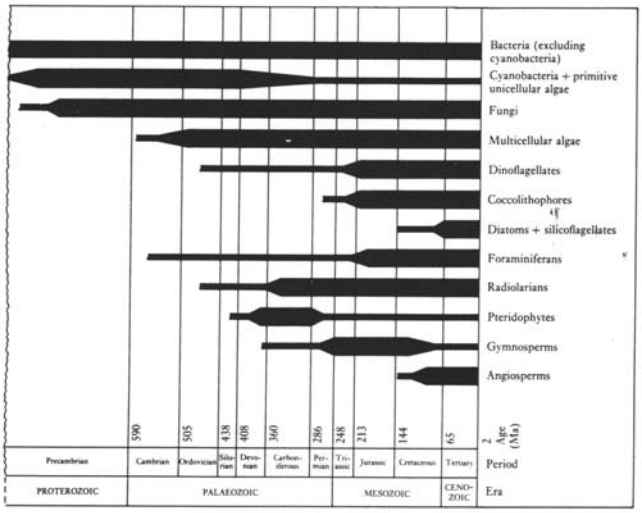

Figure 1.6 Evolution of some important contributors to sedimentary organic matter. Bar widths reflect relative abundance trends within each group of organisms.

Marine transgressions/regressions & coal/source rock formation

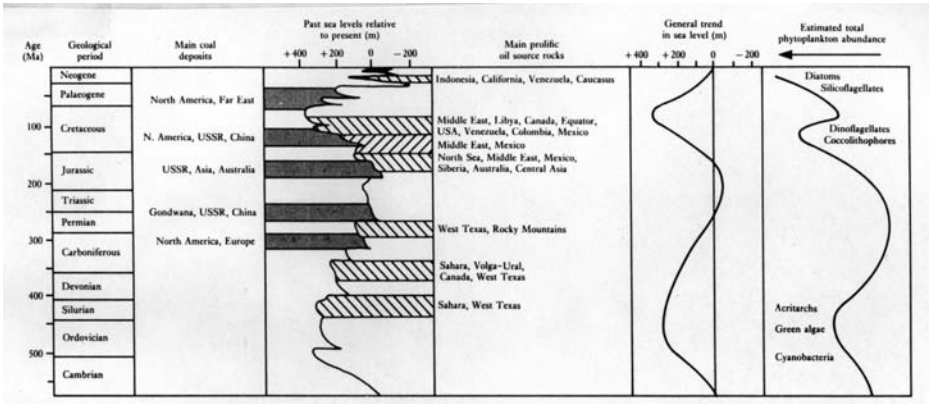

Organic matter evolution during burial and thermal maturation

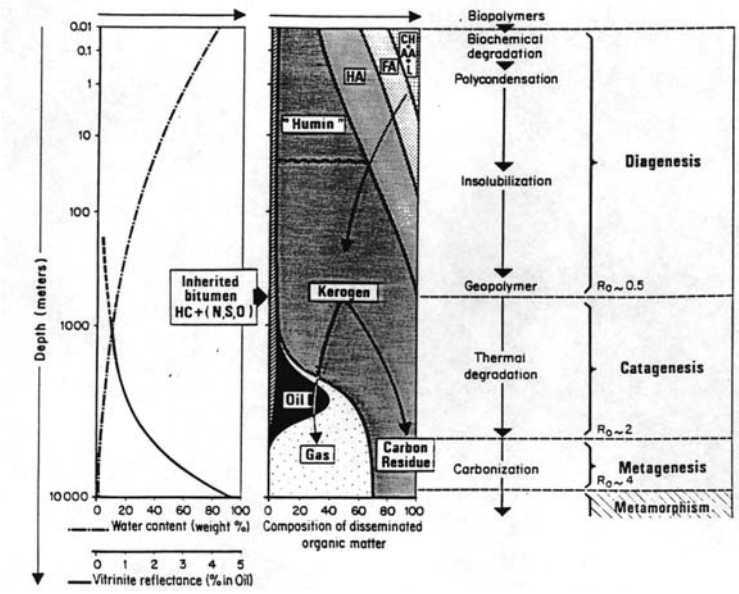

The composition of disseminated organic matter in ancient sedimentary rocks

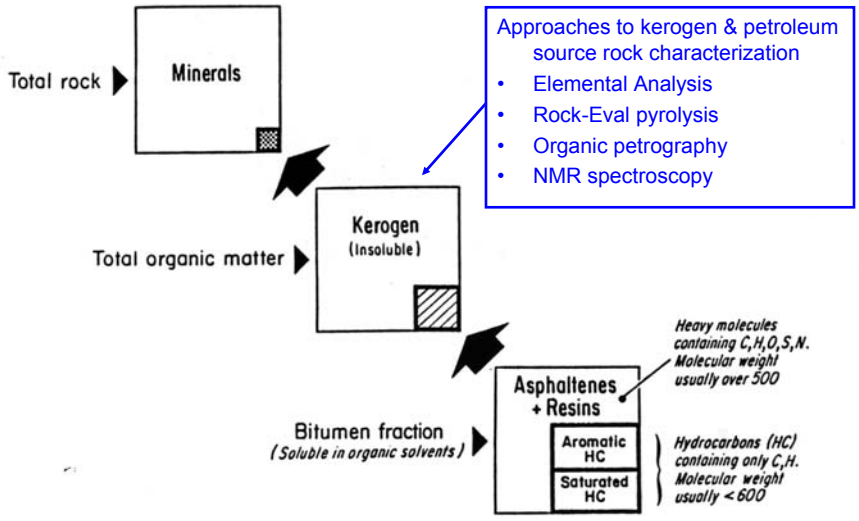

Approaches to kerogen & petroleum source rock characterization

- Elemental Analysis
- Rock-Eval pyrolysis
- Organic petrography
- NMR spectroscopy

The Van Krevelen diagram and OM evolution

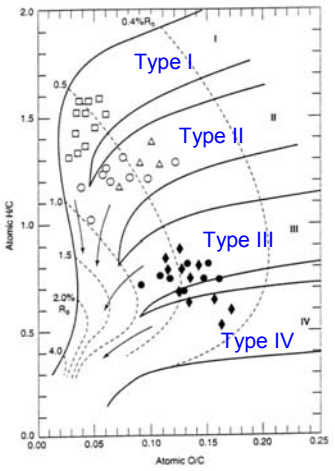

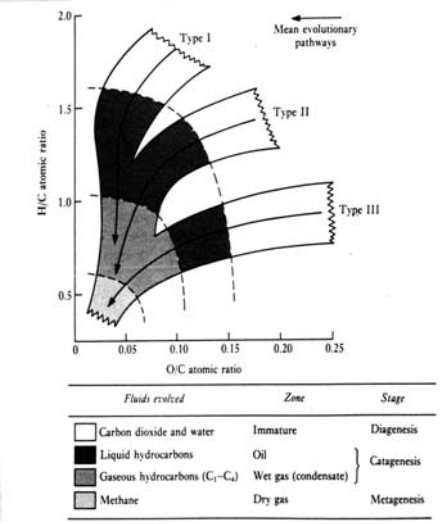

Also Type II-S, etc.

Temperature-programmed ("Rock-Eval") pyrolysis

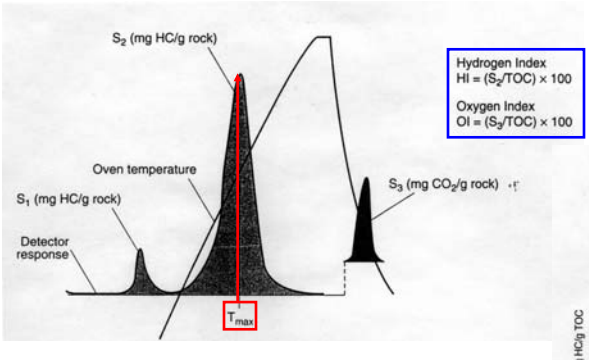

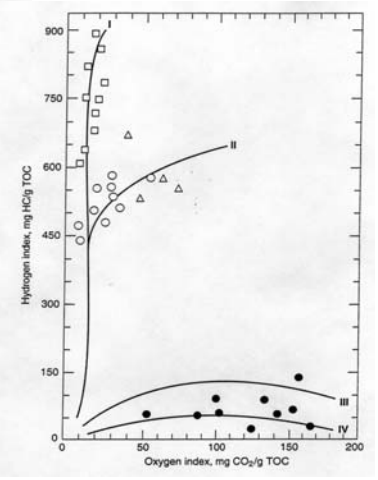

Organic petrography

	Sapropelic		*Humic*	
Coal maceral groups	Liptinite (exinite)		Vitrinite	Inertinite
Coal macerals	Alginite Cerinite[a] Sporinite Cutinite Resinite Liptodetrinite		Telinite Telocollinite Desmocollinite Vitrodetrinite	Fusinite Inertodetrinite Sclerotinite Macrinite
	Fluorescent Amorphous		Nonfluorescent Amorphous	
Kerogen Types	I	II	III	IV
H/C	1.9 to 1.0	1.5 to 0.8	1.0 to 0.5	0.6 to 0.1
O/C	0.1 to 0.02	0.2 to 0.02	0.4 to 0.02	0.3 to 0.01
Source	Marine, Lacustrine, Terrestrial		Terrestrial and Recycled	

[a]Wax.

Coals, Coal Macerals, & the Van Krevelen Diagram

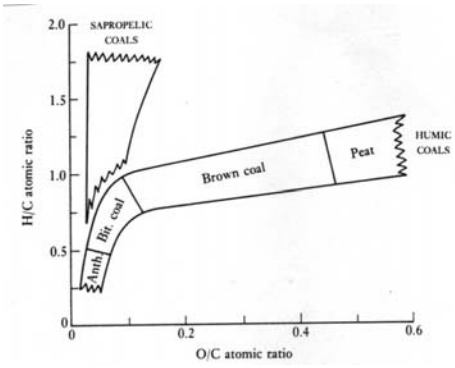

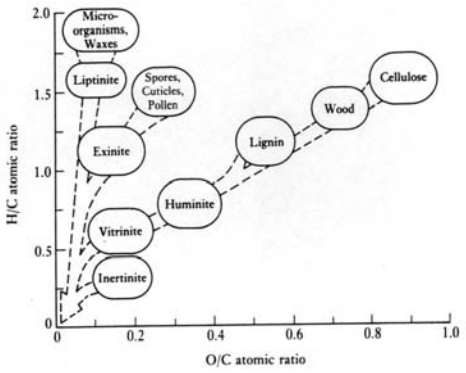

Variations in maceral reflectance

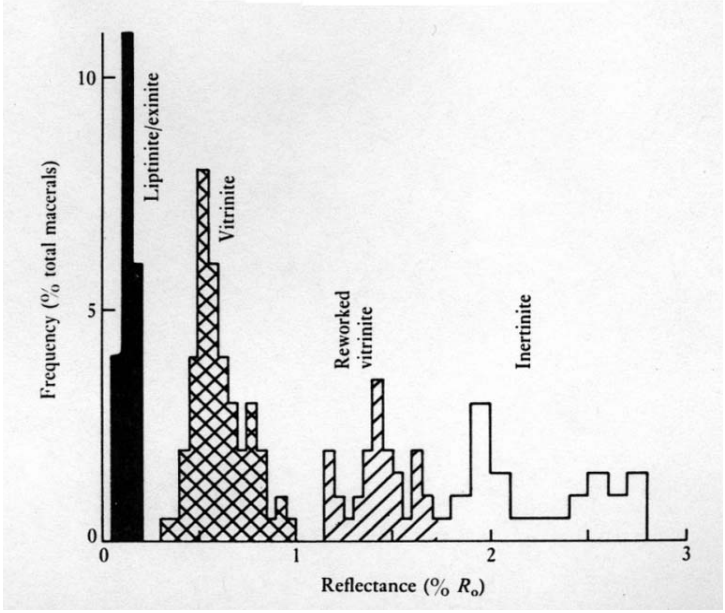

General scheme of hydrocarbon generation from source rock

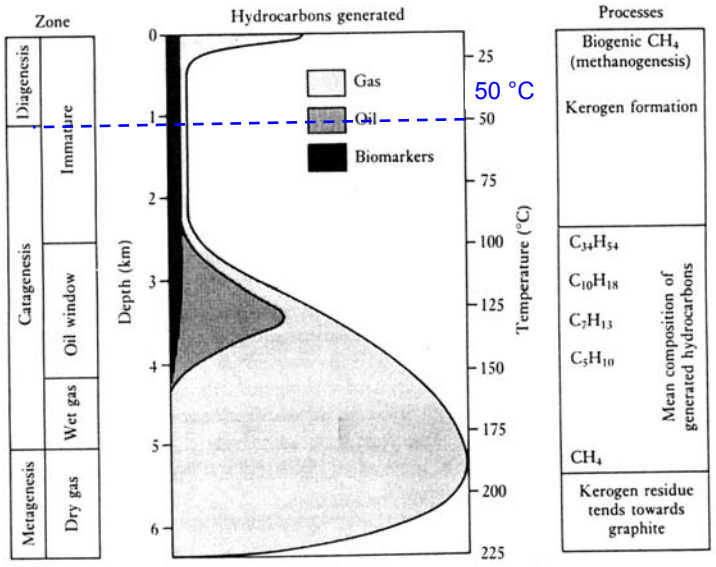

Generalized kerogen structures

Oil-generating kerogen

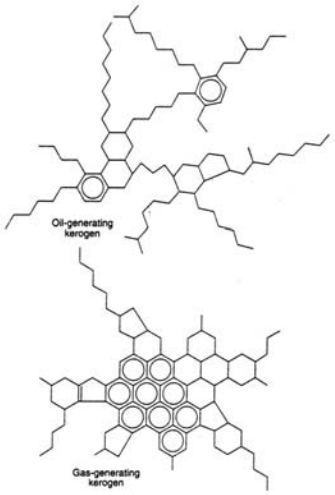

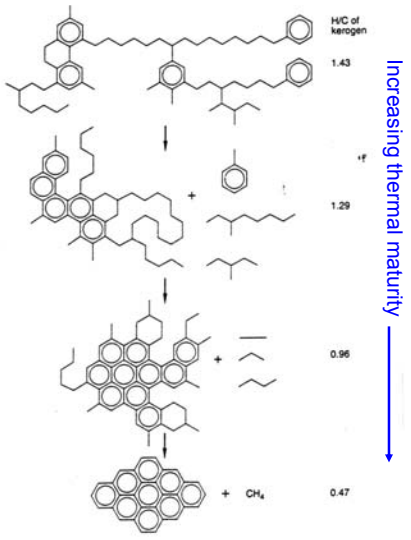

Gas-generating kerogen

Examples of hydrogen transfer reactions during catagenesis

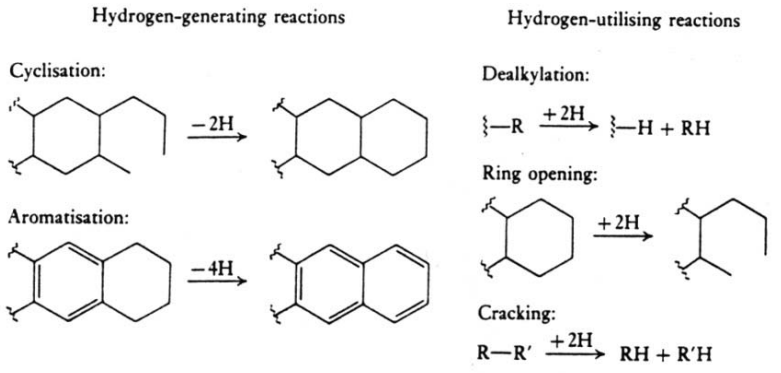

Maturity-related changes in vitrinite reflectance

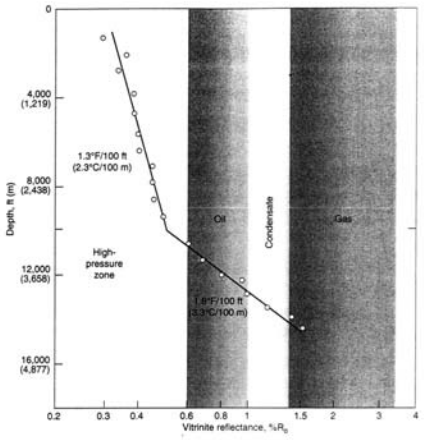

Vitrinite reflectance increase during laboratory heating

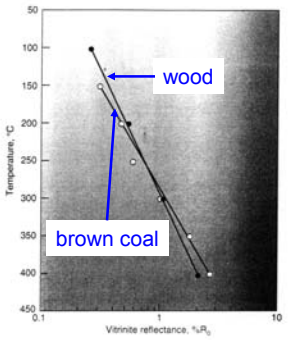

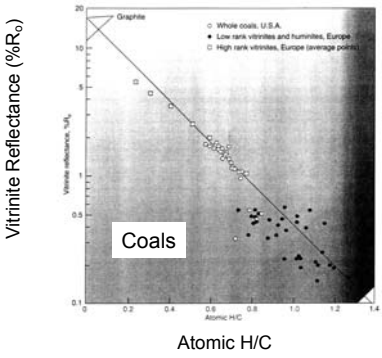

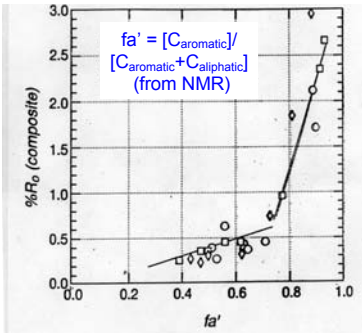

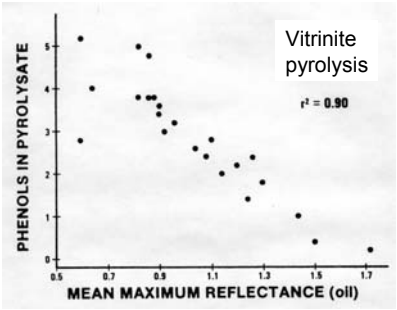

Maturity-related changes in kerogen/coal aromaticity

Typical down-core geochemical logs

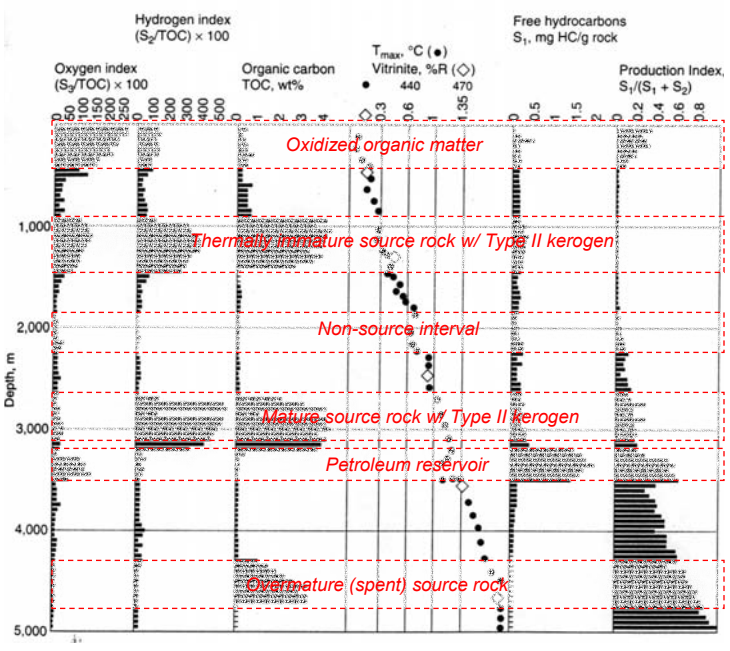

Burial history and thermal maturation

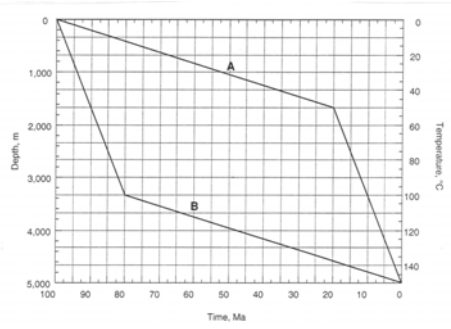

Figure 6-1
Burial history curves of hypothetical source rocks A and B overlain with a grid of isotherms at 10°C intervals.

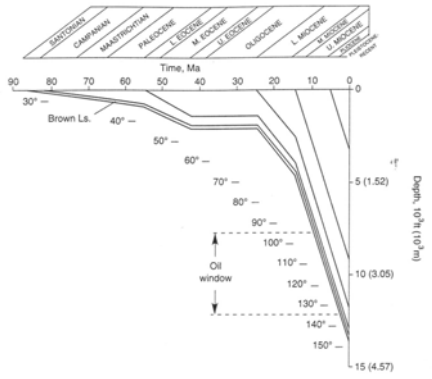

Figure 6-15
Burial history curve of the Santonian Brown Limestone in the DD83-1 well in the Gulf of Suez. [Chowdhary and Taha 1987]

Influence of sulfur on the timing of petroleum generation

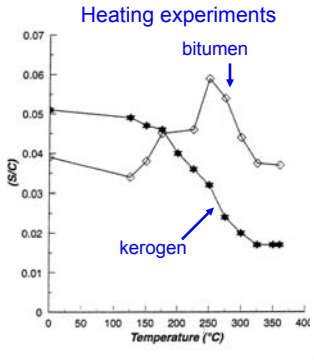

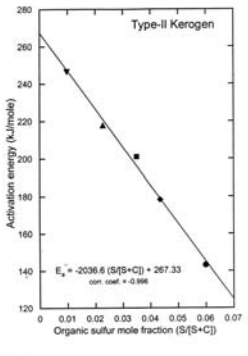

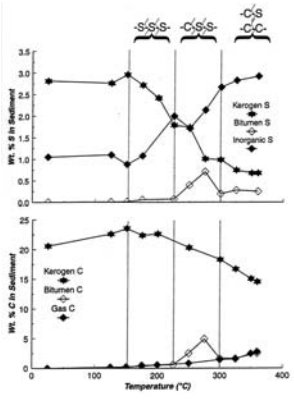

The composition of petroleum

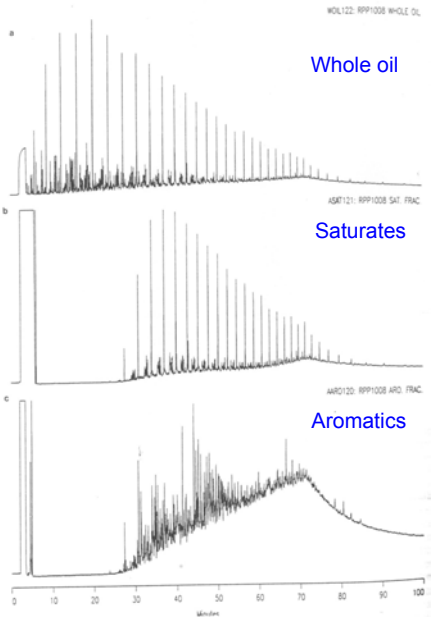

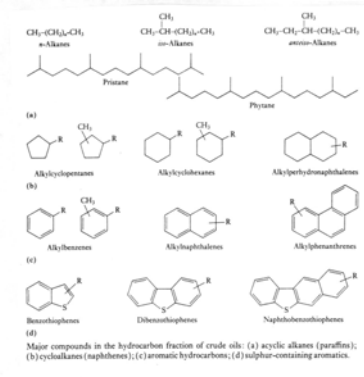

Major compounds in the hydrocarbon fraction of crude oils: (a) acyclic alkanes (paraffins); (b) cycloalkanes (naphthenes); (c) aromatic hydrocarbons; (d) sulphur-containing aromatics.

Biological Marker Concentrations in Weight Percent of Crude Oil

n-paraffins	16	Triaromatic steroids	0.1
Acyclic isoprenoids	6	Monoaromatic steroids	0.15
Pristane + phytane	0.5	C_{29} monoaromatic steroids	0.01
Hopanes	0.3	Benzohopanes	0.03
$17\alpha(H)C_{30}$-hopanes	0.02	Aromatic secohopanes	0.02
Steranes	0.3	C_{30} aromatic secohopanes	0.003
Diasteranes	0.04		

Note: Based on data for several oils from the literature plus personal communications from P. Albrecht and from J. M. Moldowan (1990).

Petroleum distillates

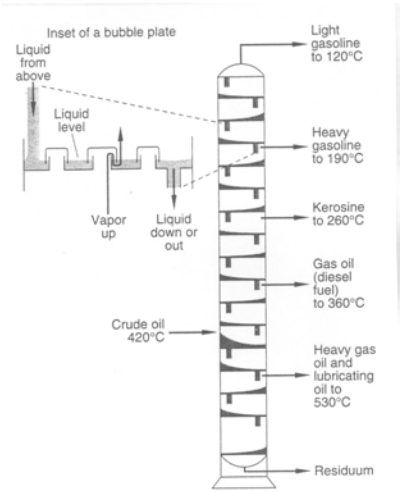

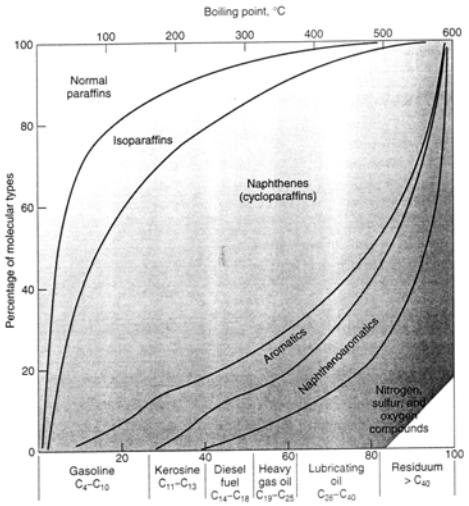

Molecular Thermal Maturity parameters

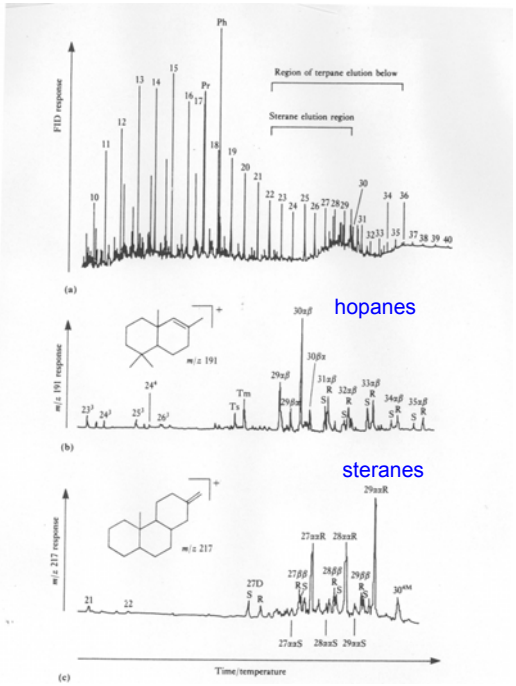

Reaction pathways for sterols

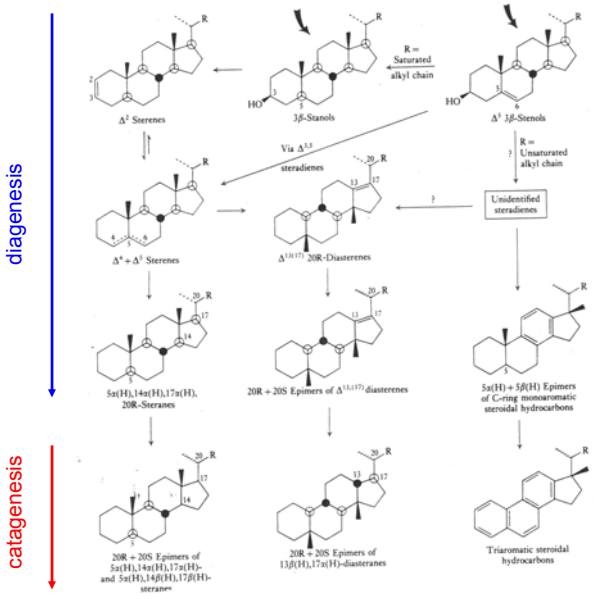

Biomarker isomerization

Biologically produced epimer

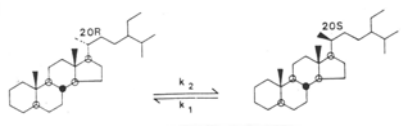

Geologically stable epimer

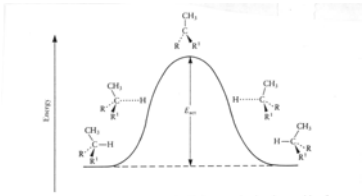

Energy profile for epimerisation at an acyclic chiral centre, showing the transition from a tetrahedrally bonded carbon atom to a trigonal planar geometry in the intermediate (E_{act} = activation energy).

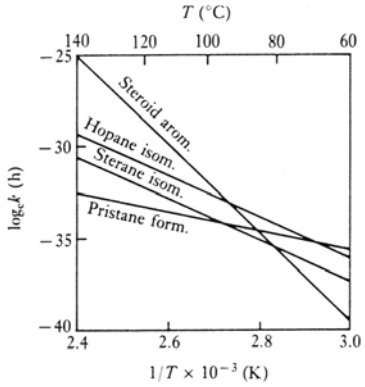

Biomarker maturity parameters

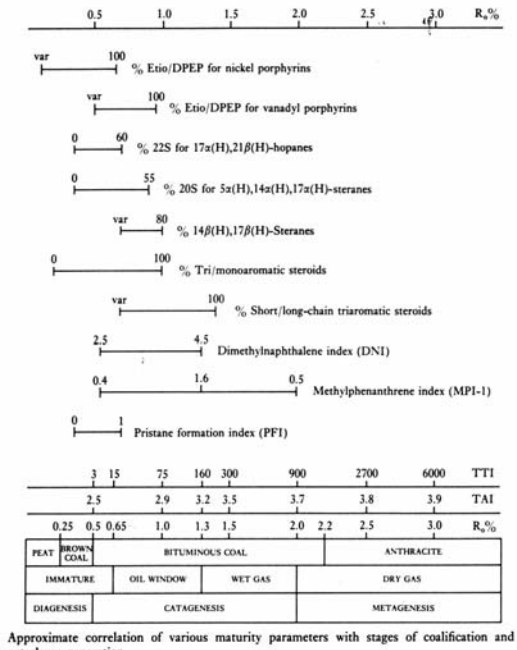

Approximate correlation of various maturity parameters with stages of coalification and petroleum generation.

Simulating petroleum generation in the laboratory

Artificial maturation of Kimmeridge shale

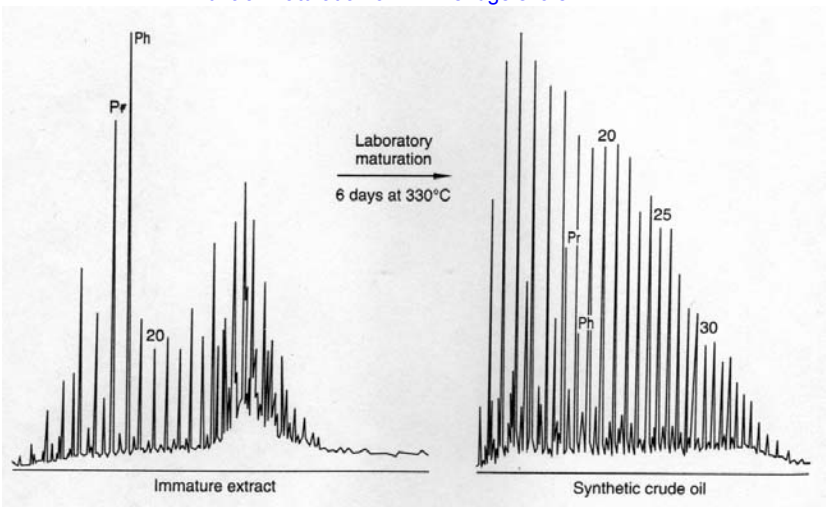

Petroleum explusion, migration and accumulation

Anticlinal trap

Fault trap

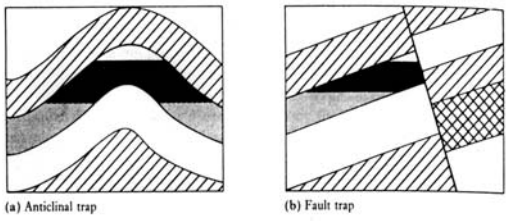

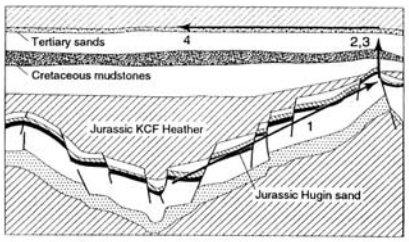

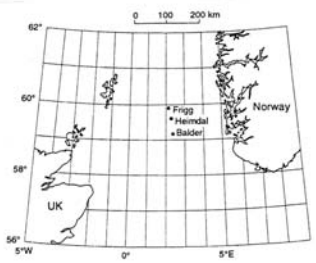

Fig. 1. Location map.

Molecular proxies of oil migration

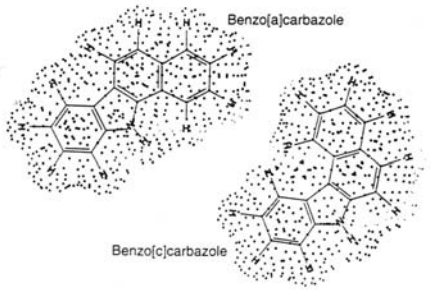

FIG. 1 Connolly dot surface plots[28] of benzo[a]carbazole and benzo[c] carbazole. The molecules are oriented with the effective dipole horizontal, the molecular electrostatic potential and partial charges ranging from negative values associated with parts of the nitrogen-bearing ring system (purple and blue) to positive partial charges and molecular electrostatic potentials associated with the pyrrolic hydrogen atom adjacent to the nitrogen atom in the molecule (red).

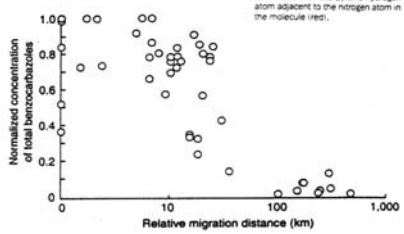

FIG. 3 Variation in the relative concentration of benzocarbazoles as a function of relative migration distance for oils in data sets 1–5 (see Fig. 2 legend) and oils from the Miller Field—all originating from marine source rocks rich in type II organic matter. The Miller field data was generated using the procedure described for data sets 1, 2 and 3. The migration distances for the Miller Field oils are measured from the main fill point of the structure. To facilitate comparison, the concentrations for each data set have been normalized to that of the oil in each data set with the highest concentration of benzo[a]carbazole.

Subsurface biodegradation of petroleum

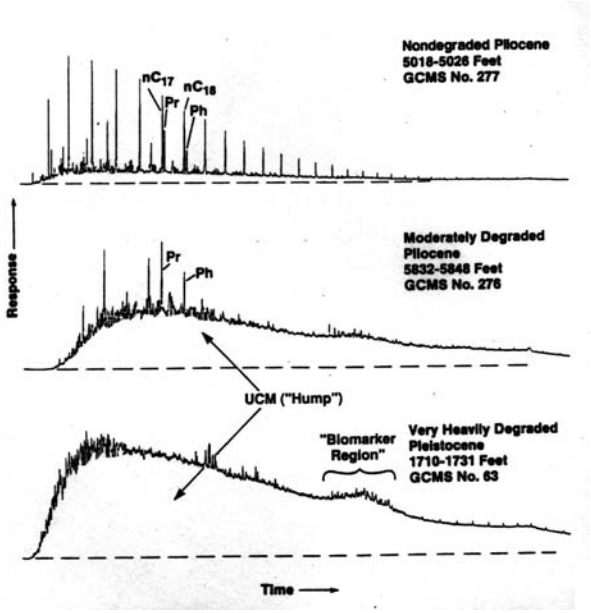

The Global Organic Carbon Cycle (ca. 1950)

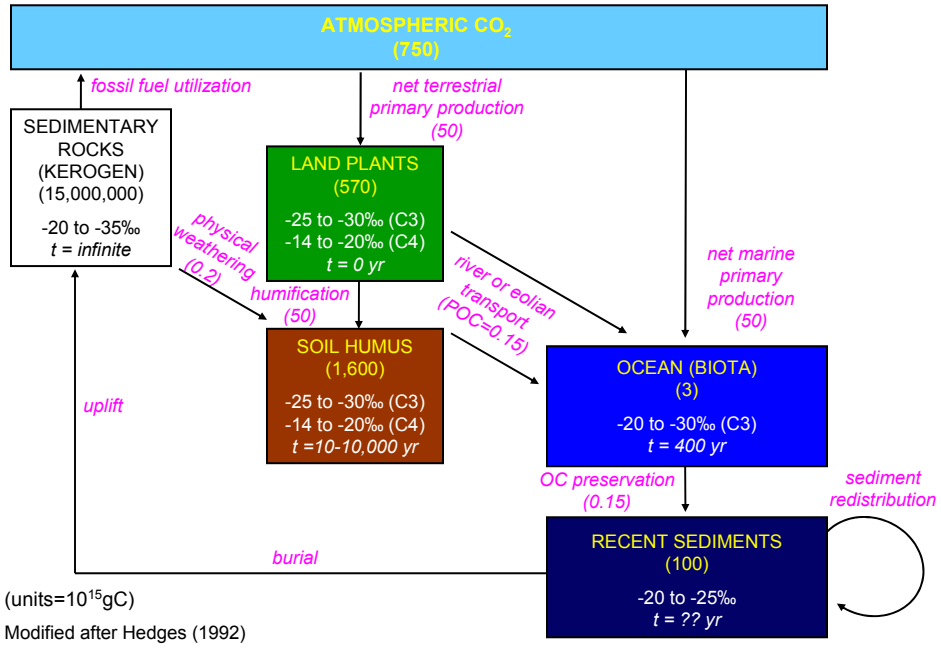

^{14}C-dead living biomass: Evidence for microbial assimilation of kerogen during shale weathering

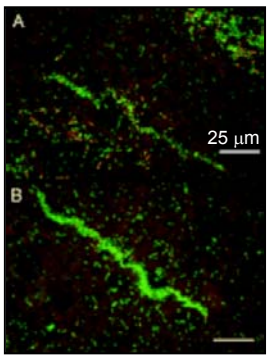

PLFA	$\Delta^{14}C$	$F_{ancient\ carbon}$	$\delta^{13}C$
$C_{16:0}$	-711	0.744	-25.5
$C_{18:0}$	-773	0.802	-26.2
$C_{18:1}+C_{18:2}$	-882	0.901	-26.5
cyc-$C_{17:0}$+cyc-$C_{19:0}$	-922	0.937	-26.9
Kerogen	-990		-29.5

Petsch et al, 2001, Science, 292, 1127-1128